Wave attractors and the asymptotic dissipation rate of tidal disturbances

By GORDON I. OGILVIE

Department of Applied Mathematics and Theoretical Physics, University of Cambridge,
Centre for Mathematical Sciences, Wilberforce Road, Cambridge CB3 0WA, UK and
Institute of Astronomy, University of Cambridge, Madingley Road, Cambridge CB3 0HA, UK

Linear waves in bounded inviscid fluids do not generally form normal modes with regular eigenfunctions. Examples are provided by inertial waves in a rotating fluid contained in a spherical annulus, and internal gravity waves in a stratified fluid contained in a tank with a non-rectangular cross-section. For wave frequencies in the ranges of interest, the inviscid linearized equations are spatially hyperbolic and their characteristic rays are typically focused onto wave attractors. When these systems experience periodic forcing, for example of tidal origin, the response of the fluid can become localized in the neighbourhood of a wave attractor. In this paper, I define a prototypical problem of this form and construct analytically the long-term response to a periodic body force in the asymptotic limit of small viscosity. The vorticity of the fluid is localized in a detached shear layer close to the wave attractor in such a way that the total rate of dissipation of energy is asymptotically independent of the viscosity. I further demonstrate that the same asymptotic dissipation rate is obtained if a non-viscous damping force is substituted for the Navier–Stokes viscosity. I discuss the application of these results to the problem of tidal forcing in giant planets and stars, where the excitation and dissipation of inertial waves may make a dominant, or at least important, contribution to the orbital and spin evolution.

1. Introduction

Geophysics and astrophysics give rise to problems involving waves in axisymmetric rotating fluid bodies. The fluid outer core of the Earth supports inertial waves, for which the Coriolis effect provides the restoring force. Such waves have been tentatively identified in gravimetric data and related to theoretical work as well as laboratory experiments (e.g. Aldridge & Lumb 1987). Helioseismology uses the observed frequencies of solar oscillations to deduce the internal structure and rotation of the Sun, while asteroseismology applies related techniques to distant stars (e.g. Christensen-Dalsgaard 2002). Waves in astrophysical accretion disks have been studied because of their important role in the interaction of a planet or other satellite with the disk in which it forms (e.g. Goldreich & Tremaine 1980), and also in an attempt to explain observed quasi-periodic oscillations from accreting white dwarfs, neutron stars and black holes (e.g. Kato 2001). Some of these problems involve free modes of oscillation that may grow through mechanisms of overstability or may be excited by turbulent noise. Tidal interactions between orbiting and spinning bodies, however, involve an almost strictly periodic forcing of waves.

After the linearized wave equations governing the dynamics of the fluid are reduced by Fourier analysis in time and azimuth, there results a two-dimensional problem for the spatial structure of the wave in the meridional plane (see Appendix A). In the absence of dissipative effects such as viscosity, this problem may have either elliptic or hyperbolic character depending on the frequency of the wave. A mixed-type problem may also occur if the character of the equations changes from one part of the body to another. Typically, hyperbolic character occurs when the wave frequency (Doppler-shifted, in the case of a non-axisymmetric wave, into the frame rotating with the local fluid) is small, in the range of inertial and gravity waves rather than acoustic waves. When a hyperbolic system of equations is posed in a finite region with physical boundary conditions on a closed surface, rather than the mathematically canonical Cauchy boundary conditions on an open surface, the problem can be regarded as ill-posed and generally does not possess a regular solution. This property presents a serious difficulty when one seeks the response of a body to low-frequency tidal forcing. (In accretion discs, where the systematic shear causes a strong Doppler shift of the frequency of non-axisymmetric waves, the equations typically have hyperbolic character in the vicinity of the corotation resonance.)

It is possible to sidestep this issue in certain problems of special symmetry where a separation of variables can be applied. For example, in a spherically symmetric non-rotating star the linearized equations can be projected onto spherical harmonics and the problem reduced to a system of ordinary differential equations in the radial direction. Most treatments of tides in stars and giant planets have used this approach (e.g. Zahn 1970), or have included the Coriolis force within the so-called 'traditional approximation' (in which only the radial component of the angular velocity is considered), which also permits a separation of variables (e.g. Ioannou & Lindzen 1993; Savonije & Witte 2002). The simplest problems involving inertial waves, featuring an incompressible fluid in a full spherical, spheroidal or cylindrical container, can also be solved by separation of variables and appear to possess complete sets of normal modes with regular eigenfunctions, even in the absence of viscosity (e.g. Greenspan 1968; Zhang, Liao & Earnshaw 2004).

Unfortunately, the approximation of a non-rotating star is rarely valid in problems of tidal forcing. The tidal frequencies are linear combinations of the orbital and spin frequencies with small integer coefficients, apart from small corrections due to any precessional effects. In most problems of interest, the frequencies of the most important tidal components are smaller in magnitude than twice the spin frequency of the body, and the Coriolis force cannot be neglected (Ogilvie & Lin 2004). The traditional approximation is valid only in stably stratified regions where the tidal frequency is much less than the buoyancy frequency, and does not apply in convective regions of stars or giant planets where the buoyancy frequency is essentially zero. In such regions, the wave equations are hyperbolic in character, describing pure inertial waves, and cannot be solved by separation of variables. Numerical solutions of the two-dimensional problem were obtained by Savonije, Papaloizou & Alberts (1995) and Savonije & Papaloizou (1997) in the case of an early-type star with a small convective core and, more recently, by Ogilvie & Lin (2004) in the case of a giant planet with an extended convective region.

Numerical studies have revealed the intricate structure of inertial waves in an incompressible rotating fluid contained in a spherical annulus (Hollerbach & Kerswell 1995; Rieutord & Valdettaro 1997). In order to find normal modes it is necessary to include a viscosity so that the problem becomes of elliptic character and is mathematically regularized. As the viscosity tends to zero the eigenfunctions become

increasingly localized in the neighbourhood of singular linear structures known as wave attractors, as described in greater detail by Rieutord, Georgeot & Valdettaro (2001) and Rieutord, Valdettaro & Georgeot (2002). A wave attractor can be understood as a limit cycle towards which the characteristic rays of the inviscid wave equation are focused as they reflect repeatedly from the boundaries of the container. Unlike the case of a full sphere, it appears that inertial waves in a spherical annulus do not possess regular eigenfunctions in the absence of viscosity, apart from the exceptional 'r modes' or 'toroidal modes' which involve no radial motion. The presence of an inner core introduces a complexity into the reflection patterns of the characteristic rays and causes them to be focused onto wave attractors. The existence and importance of these closed ray circuits in spherical shells have been known for some time (Stern 1963; Bretherton 1964) and many features of this problem were understood before the advent of high-resolution numerical calculations (Stewartson & Rickard 1969; Stewartson 1972).

Wave attractors have also been studied for internal gravity waves. In a notable experiment, Maas *et al.* (1997) applied a periodic forcing to a narrow tank containing a stratified salt solution. For wave frequencies smaller in magnitude than the uniform buoyancy frequency of the fluid, the characteristic rays of the inviscid wave equation are straight lines with a definite angle of inclination depending on the frequency. In an upright rectangular tank, the rays would propagate around the container ergodically or, for special frequencies related to the rational numbers, would close after a finite number of reflections. By making one of the sidewalls sloping, Maas *et al.* (1997) introduced a wave attractor, in this case an inclined rectangle, into the problem (Maas & Lam 1995). Their experiment indicates that the forced response is localized in the neighbourhood of the attractor, and this concentration ultimately leads to secondary effects such as mixing. Inertial waves in a rotating tank of similar shape have also been studied by Maas (2001) and Manders & Maas (2003).

There is a close analogy between these problems. The relation between the tank with the sloping sidewall and the upright rectangular tank is similar to the relation between the spherical annulus and the full sphere. In each case, rays in the geometrically simpler container (rectangular tank or full sphere) propagate ergodically or, for special frequencies, form periodic orbits. The inviscid wave equation admits regular eigenfunctions for a countable set of frequencies, which may or may not be those for which the rays form periodic orbits. In the geometrically more complicated, but more generic, containers, the rays are focused onto one or more wave attractors for almost all wave frequencies, and the inviscid wave equation does not admit regular eigenfunctions.

In problems of tidal forcing it is of great interest to know how the total dissipation rate varies with the forcing frequency, as this determines the rate of secular evolution of tidally interacting systems. When the viscosity is small, systems that possess regular inviscid normal modes can be expected to exhibit a strong resonant amplification of the dissipation rate in the vicinity of the eigenfrequencies, but very small dissipation elsewhere. Although the eigenfrequencies may be everywhere dense in some interval, the smooth forcing will have a significant overlap only with a few of the lowest-order modes. In contrast, wave attractors have a structural stability, and exist in intervals of frequency that depend on the geometry rather than the viscosity. Systems possessing wave attractors can be expected to exhibit a richer response with significant dissipation occurring over extended ranges of frequency.

The purpose of this paper is to analyse the linear response of such systems to periodic forcing in the low-viscosity limit relevant to the geophysical and astrophysical

applications. I work with simplified model problems, but also explain how they are related to the original systems. The main result is a validation of the conjecture of Ogilvie & Lin (2004) that, in problems where a wave attractor occurs, the total dissipation rate tends to a non-zero value that is independent of both the magnitude and the form of the small-scale damping process of the waves. This outcome differs significantly from problems that possess regular inviscid normal modes and is of primary importance for tidally interacting systems. The analysis presented here provides a method of calculating the asymptotic dissipation rate and also describes the spatial form of the forced disturbance.

The remainder of this paper is organized as follows. In §2, I briefly describe the problem of forced internal gravity waves as a definite example of the system under consideration. I define a prototypical problem in §3 and construct the asymptotic solution in the limit of small viscosity. In §4, I adapt the analysis to a related problem in which the damping mechanism is not of a viscous nature. I present the results of direct numerical calculations in §5 and compare these with the asymptotic theory. A concluding discussion is found in §6.

2. Forced internal gravity waves

In this section, I outline the preliminary analysis for forced internal gravity waves in a narrow tank. This is essentially identical to the problem studied by Maas *et al.* (1997) except that a vortical body force is assumed rather than a parametric forcing.

Consider a fluid initially at rest in a gravitational field $-g\,\boldsymbol{e}_z$ and with a uniform temperature gradient $\beta\,\boldsymbol{e}_z$, where (x, y, z) are Cartesian coordinates. In the Boussinesq approximation, the linearized equations for the velocity $\boldsymbol{u}$ and the temperature perturbation θ are (Chandrasekhar 1961)

$$\frac{\partial \boldsymbol{u}}{\partial t} = -\nabla \varpi + g\alpha\theta\,\boldsymbol{e}_z + \nu\nabla^2\boldsymbol{u} + \boldsymbol{a}, \tag{2.1}$$

$$\frac{\partial \theta}{\partial t} = -\beta u_z + \kappa\nabla^2\theta, \tag{2.2}$$

$$\nabla \cdot \boldsymbol{u} = 0, \tag{2.3}$$

where ϖ is the pressure perturbation divided by the reference density, α is the coefficient of expansion, ν is the kinematic viscosity and κ is the thermal diffusivity. The fluid is excited by an external body force $\boldsymbol{a}$ per unit mass.

Consider a two-dimensional problem, approximately representative of the situation in a narrow tank, in which $u_y = a_y = 0$ and all quantities are independent of y. The velocity is described by a streamfunction ψ such that

$$u_x = -\frac{\partial \psi}{\partial z}, \qquad u_z = \frac{\partial \psi}{\partial x}. \tag{2.4}$$

I focus on the limit of large Prandtl number in which κ can be neglected (except in thermal boundary layers, which are of negligible thickness compared to the viscous boundary layers). In reality, the Prandtl number of water exceeds 10 for temperatures below about $10\,^\circ\mathrm{C}$, so this limit may be of some relevance for laboratory experiments or for terrestrial tides confined in oceanic basins.

When considering the long-term response to a periodic force with (real) angular frequency ω, all perturbation quantities may be assumed to have the form

$$\boldsymbol{u} = \mathrm{Re}[\tilde{\boldsymbol{u}}(x, z)\,\mathrm{e}^{-\mathrm{i}\omega t}], \tag{2.5}$$

etc. Eliminating $\tilde{\varpi}$ and $\tilde{\theta}$, one obtains the linearized vorticity equation in the form

$$\mathrm{i}\omega\nabla^2\tilde{\psi} = \frac{\mathrm{i}N^2}{\omega}\frac{\partial^2\tilde{\psi}}{\partial x^2} - \nu\nabla^4\tilde{\psi} + f, \qquad (2.6)$$

where $N^2 = g\alpha\beta$ is the square of the buoyancy frequency and

$$f = \frac{\partial\tilde{a}_x}{\partial z} - \frac{\partial\tilde{a}_z}{\partial x} \qquad (2.7)$$

is the y-component (and only non-vanishing component) of the vorticity forcing $\nabla\times\tilde{a}$. (It may be noted that tidal forcing always derives from a potential and therefore has no curl. Nevertheless, the dynamical tide in a body of non-uniform density, or one with a free surface, does experience a vortical effective forcing as explained in Appendix B.)

With rigid walls, the boundary conditions are

$$\tilde{\psi} = 0, \qquad \boldsymbol{n}\cdot\nabla\tilde{\psi} = 0, \qquad (2.8)$$

where $\boldsymbol{n}$ is the outward normal vector on the boundary. The time-averaged dissipation rate (per unit length in the y-direction) is

$$D = \tfrac{1}{2}\iint \nu|\nabla^2\tilde{\psi}|^2 \,\mathrm{d}x\,\mathrm{d}z, \qquad (2.9)$$

where the integral extends over the area of the container in the (x, z)-plane. Using (2.6) and the boundary conditions, one can relate the dissipation to an overlap integral between the vorticity forcing and the streamfunction in the form

$$D = \tfrac{1}{2}\operatorname{Re}\iint \tilde{\psi}^* f \,\mathrm{d}x\,\mathrm{d}z. \qquad (2.10)$$

The spectrum of internal gravity waves lies in the interval $-N < \omega < N$. In this range of frequencies, the inviscid version of (2.6), with $\nu = 0$, involves a hyperbolic operator

$$\omega^2\nabla^2 - N^2\frac{\partial^2}{\partial x^2} = \omega^2\frac{\partial^2}{\partial z^2} - (N^2 - \omega^2)\frac{\partial^2}{\partial x^2}. \qquad (2.11)$$

The characteristics of the inviscid equation are straight lines with slopes $\pm\omega(N^2 - \omega^2)^{-1/2}$ that depend on the wave frequency. The occurrence of wave attractors in containers of various shapes has been illustrated by Maas *et al.* (1997).

3. A prototypical problem and its asymptotic solution

3.1. *Definition of the problem*

In this section, I slightly abstract the above problem and define a prototypical model problem that is very closely related, but marginally simpler to solve. Consider the equation

$$\mathrm{i}\frac{\partial^2\psi}{\partial x\,\partial y} + \epsilon^3\nabla^4\psi = f, \qquad (3.1)$$

for an unknown function $\psi(x, y)$ in a domain $\mathscr{D}\subset\mathbf{R}^2$, with boundary conditions

$$\psi = 0, \qquad \boldsymbol{n}\cdot\nabla\psi = 0 \qquad \text{on }\partial\mathscr{D}. \qquad (3.2)$$

Here, $\epsilon \ll 1$ is a small dimensionless parameter, $f(x, y)$ is a given complex-valued function and $\boldsymbol{n}$ is the outward normal vector on $\partial\mathscr{D}$.

As suggested by §2, one can think of ψ as the streamfunction of a two-dimensional flow of an incompressible fluid subject to no-slip boundary conditions. The viscosity of the fluid is proportional to ϵ^3 and the curl of the body force is proportional to f. The limit $\epsilon \ll 1$ corresponds to the Reynolds number being large. The problem is linearized and a harmonic time-dependence of all quantities has been assumed. The fluid has a restoring force such as buoyancy or the Coriolis force. In fact, the inviscid part of the problem of forced internal gravity waves considered above can be rendered exactly in this form by a linear transformation of the coordinates, depending on the wave frequency, that maps the sloping characteristics onto horizontal and vertical lines. In the process, the viscous ∇^4 operator is slightly modified, although this has essentially no practical consequences.

Consider the inviscid version of (3.1), obtained by setting $\epsilon = 0$ and abandoning the no-slip boundary condition $\boldsymbol{n} \cdot \nabla \psi = 0$. The inviscid equation is hyperbolic and its characteristics are horizontal and vertical lines. In general, the inviscid problem is mathematically ill-posed and does not possess a regular solution. Instead, one must consider the limit $\epsilon \to 0$ of the viscous problem.

The time-averaged energy dissipation rate may be defined as

$$D = \tfrac{1}{2} \int_{\mathscr{D}} \epsilon^3 |\nabla^2 \psi|^2 \, \mathrm{d}A. \tag{3.3}$$

Using (3.1) and the boundary conditions (3.2), one can relate the dissipation to an overlap integral between the vorticity forcing and the streamfunction in the form

$$D = \tfrac{1}{2} \mathrm{Re} \int_{\mathscr{D}} \psi^* f \, \mathrm{d}A. \tag{3.4}$$

The problem at hand is to determine how D depends on ϵ in the limit $\epsilon \to 0$ (and also on f and $\mathscr{D}$ if these are varied).

3.2. *Ray circuits and the wave attractor*

A *ray segment* consists of a horizontal or vertical line segment connecting two points of $\partial \mathscr{D}$ (*vertices*) and lying wholly in $\mathscr{D}$. A *ray circuit* consists of a connected set of consecutive ray segments and represents the propagation of a wave characteristic around the container. Typically, a ray circuit will be of infinite length. Exceptionally, a circuit that closes on itself after a finite number of reflections is a *periodic orbit*.

In principle, the domain $\mathscr{D}$ may contain any number of periodic orbits. I consider the case in which $\mathscr{D}$ contains exactly one periodic orbit and the orbit is simple (i.e. a rectangle). Without loss of generality, one may place the origin of coordinates at the bottom left-hand corner of the rectangle so that the corners $OABC$ are at $(0, 0)$, $(X, 0)$, (X, Y) and $(0, Y)$ with $X, Y > 0$. I label the segments 1, 2, 3, 4 in the order OA, AB, BC, CO. Let the slopes of the boundary at the four corners be $s_A = t_1$, $s_B = -t_2^{-1}$, $s_C = t_3$ and $s_O = -t_4^{-1}$. Then $t_j > 0$ is the tangent of the angle between the 'incident' ray (in the positive sense $OABC$) and the boundary at the end of segment j.

For rays close to the periodic orbit, the boundary may be represented locally by linear approximations

$$\left.\begin{aligned}
y &\approx t_1(x - X) & &\text{near } A, \\
y &\approx -t_2^{-1}(x - X) + Y & &\text{near } B, \\
y &\approx t_3 x + Y & &\text{near } C, \\
y &\approx -t_4^{-1} x & &\text{near } O.
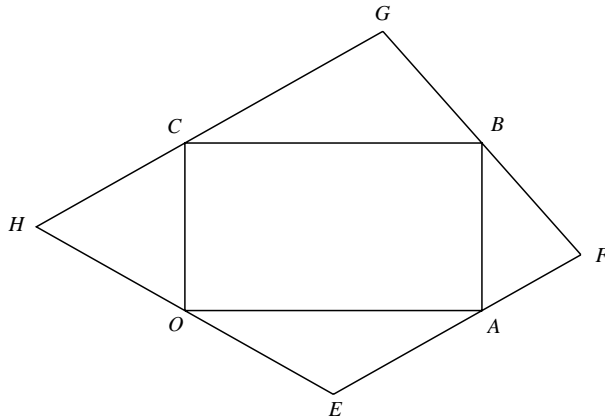\end{aligned}\right\} \tag{3.5}$$

FIGURE 1. Example of a quadrilateral domain containing a unique wave attractor.

The local approximate mapping of vertices defined by the ray propagation (in the positive sense $OABC$) is then

$$(-t_4 y, y) \mapsto (t_1^{-1} y + X, y)$$
$$\mapsto (t_1^{-1} y + X, -t_1^{-1} t_2^{-1} y + Y)$$
$$\mapsto (-t_1^{-1} t_2^{-1} t_3^{-1} y, -t_1^{-1} t_2^{-1} y + Y)$$
$$\mapsto (-t_1^{-1} t_2^{-1} t_3^{-1} y, t_1^{-1} t_2^{-1} t_3^{-1} t_4^{-1} y). \qquad (3.6)$$

On each loop, therefore,

$$(-t_4 y, y) \mapsto \alpha^{-1}(-t_4 y, y), \qquad \alpha = t_1 t_2 t_3 t_4. \qquad (3.7)$$

It may be expected that $\alpha \neq 1$ in a typical asymmetric container. The periodic orbit is then attracting, and focuses rays propagating either in a positive sense (if $\alpha > 1$) or in a negative sense (if $0 < \alpha < 1$). I assume without loss of generality that $\alpha > 1$ (the case $0 < \alpha < 1$ can be obtained by a reflection of the problem). The focusing direction is then $OABC$ and α is the focusing power of the attractor.

A particularly useful illustrative example is provided by a quadrilateral container (figure 1). The quadrilateral is defined uniquely by specifying the rectangle $OABC$ and the four tangents t_j. It can be shown that the wave attractor is unique. All ray circuits other than the attractor itself converge towards the attractor at either end. I assume that this property holds in the domain $\mathcal{D}$.

The attractor divides the boundary into two zones, one consisting of OEA together with BGC and the other consisting of AFB together with CHO. Ray circuits other than the attractor itself have all their vertices in one zone or the other. Therefore the attractor has two 'sides' to it, and any ray circuit converges towards the attractor from the same side at either end.

For rays near the attractor one can measure the distance from the attractor using the y-coordinates of the appropriate vertices (those near O). The entire bundle of rays associated with one side of the attractor (e.g. the 'positive' side $y > 0$) can be labelled using a variable $\theta^+ \in [0, 1)$ defined as follows. One starts a ray at a vertex very close to O and with y-coordinate $y = \alpha^{-n-\theta^+}$ for some arbitrarily large positive integer $n \gg 1$. The ray is followed in the negative sense as it spirals away from the attractor. Eventually, it turns around and converges towards the attractor again, having vertices

very close to O with y-coordinates $y \sim \alpha^{-n-\Theta^+(\theta^+)}$, $n \gg 1$. This mapping between one end of a ray circuit and the other defines a function $\Theta^+(\theta^+)$, with $\Theta^+ \in [0, 1)$.

The variable θ^+ is periodic in nature ($\theta^+ = 1$ is identified with $\theta^+ = 0$) since the ray bundle wraps around itself. The function $\Theta^+(\theta^+)$ can be considered topologically as a map of the circle onto itself. Owing to the reversibility of the ray circuit, it has the self-inverting property $\Theta^+(\Theta^+(\theta^+)) = \theta^+$, which will be used later.

For the negative side $y < 0$ of the attractor, there is a similar variable θ^- and a mapping $\Theta^-(\theta^-)$. In problems with multiple or non-simple attractors, a more complicated mapping of ray bundles is likely to exist.

3.3. Construction of an asymptotic solution

In the limit $\epsilon \to 0$, the solution divides into three regions: (i) an inner region localized near the wave attractor and consisting of a detached shear layer of width $O(\epsilon)$; (ii) an outer region consisting of most of the rest of the container; (iii) standard viscous boundary layers of width $O(\epsilon^{3/2})$ close to the walls. There are also boundary layers in the corner regions close to the vertices of the attractor.

I first simplify the problem by assuming that a particular solution for the inviscid problem can be found, i.e. a function $\hat{\psi}(x, y)$ satisfying the equation

$$i\frac{\partial^2 \hat{\psi}}{\partial x \partial y} = f \tag{3.8}$$

without regard to boundary conditions. (This can be obtained by an indefinite integration of $-if$ with respect to x and y.) The desired solution is then $\psi = \hat{\psi} + \tilde{\psi}$ where $\tilde{\psi}$ satisfies the equation

$$i\frac{\partial^2 \tilde{\psi}}{\partial x \partial y} + \epsilon^3 \nabla^4 \tilde{\psi} = -\epsilon^3 \nabla^4 \hat{\psi} \tag{3.9}$$

and the boundary conditions

$$\tilde{\psi} = -\hat{\psi}, \qquad \boldsymbol{n} \cdot \nabla \tilde{\psi} = -\boldsymbol{n} \cdot \nabla \hat{\psi}. \tag{3.10}$$

Note that f and $\hat{\psi}$ are supposed to be smooth and do not have any fine structure associated with boundary layers or shear layers. Therefore the right-hand side of (3.9) is small everywhere and will be unimportant in constructing the leading-order asymptotic solution. The inhomogeneity has effectively been transferred from the differential equation to the boundary conditions.

3.4. The outer solution

The asymptotic outer solution is simply of the form

$$\tilde{\psi} \sim \tilde{\psi}^{(out)}(x, y). \tag{3.11}$$

It satisfies the inviscid problem

$$i\frac{\partial^2 \tilde{\psi}^{(out)}}{\partial x \partial y} = 0, \tag{3.12}$$

with the boundary condition

$$\tilde{\psi}^{(out)} = -\hat{\psi}. \tag{3.13}$$

The second boundary condition is taken care of by the intervention of a standard viscous boundary layer (region (iii) mentioned above).

The general solution of (3.12) is

$$\tilde{\psi}^{(out)} = g(x) - h(y), \tag{3.14}$$

where g and h are functions to be determined. Consider two consecutive vertices, P and Q, say, of a ray circuit. If they are connected by a horizontal ray segment, they share the same value of y and therefore of $h(y)$. It follows from (3.13) and (3.14) that $g(x_Q) - g(x_P) = \hat{\psi}_P - \hat{\psi}_Q$. Similarly, for vertices connected by a vertical ray segment, $h(y_Q) - h(y_P) = \hat{\psi}_Q - \hat{\psi}_P$. Since $\hat{\psi}$ is known, a knowledge of g (or h) at any vertex would be sufficient to propagate the solution along the ray circuit. However the given boundary conditions do not provide such information.

Consider the ray circuit as described in §3.2. At each end of the circuit, the ray indefinitely repeats a loop around the attractor $OABC$. Around each loop the value of g must change by an amount

$$\delta = \hat{\psi}_O - \hat{\psi}_A + \hat{\psi}_B - \hat{\psi}_C, \tag{3.15}$$

and the value of h also changes by δ. Since $\hat{\psi}$ is smooth, one need not worry about the small variation of $\hat{\psi}$ close to the vertices of the attractor. In fact,

$$\delta = \iint \frac{\partial^2 \hat{\psi}}{\partial x \partial y} \, \mathrm{d}x \, \mathrm{d}y = -\mathrm{i} \int f \, \mathrm{d}A, \tag{3.16}$$

where the integration is over the area enclosed by the attractor. Therefore δ is independent of the choice of particular solution $\hat{\psi}$. It is also notable that if, as in §2, f is the perpendicular component of the curl of the external force per unit mass, then Stokes's theorem provides a simple relation between δ and the line integral $\oint \tilde{a} \cdot \mathrm{d}r$ of the force around the attractor.

It follows that $h(y)$ exhibits an increasingly fine structure and, in general, a logarithmic divergence as $y \to 0$. The same is true of $g(x)$ near $x = 0$ and $x = X$, and of $h(y)$ near $y = Y$. This singular behaviour of the outer solution is the reason that an inner region, in which viscosity regularizes the solution, is required. For small y, one has

$$h(\alpha^{-1}y) - h(y) \approx \delta. \tag{3.17}$$

Consider the positive side $y > 0$ first and define the variable $\tilde{y}^+ = -\ln y / \ln \alpha$, which increases by 1 on each loop. Then $h(y) \sim \tilde{h}^+(\tilde{y}^+)$ as $y \searrow 0$, with

$$\tilde{h}^+(\tilde{y}^+ + 1) - \tilde{h}^+(\tilde{y}^+) = \delta. \tag{3.18}$$

The general solution of this functional equation is

$$\tilde{h}^+(\tilde{y}^+) = \tilde{y}^+ \delta + H^+(\theta^+), \tag{3.19}$$

i.e.

$$h(y) \sim \left(-\frac{\ln y}{\ln \alpha} \right) \delta + H^+(\theta^+) \qquad \text{as } y \searrow 0, \tag{3.20}$$

where

$$\theta^+ = \tilde{y}^+ \bmod 1 = \left(-\frac{\ln y}{\ln \alpha} \right) \bmod 1 \tag{3.21}$$

is the ray-labelling variable introduced previously and H^+ is an arbitrary function with period 1. It may be expanded in a Fourier series

$$H^+(\theta^+) = \sum_{n=-\infty}^{\infty} H_n^+ e^{2n\pi i\theta^+}. \tag{3.22}$$

For the negative side of the attractor, a similar result holds, with

$$h(y) \sim \left(-\frac{\ln|y|}{\ln\alpha}\right)\delta + H^-(\theta^-) \qquad \text{as } y \nearrow 0 \tag{3.23}$$

and

$$H^-(\theta^-) = \sum_{n=-\infty}^{\infty} H_n^- e^{2n\pi i\theta^-}. \tag{3.24}$$

Now consider the total change in $h(y)$ around the ray circuit, from a vertex with $y = \alpha^{-n_1-\theta^+}$, $n_1 \gg 1$, to a vertex with $y \sim \alpha^{-n_2-\Theta^+(\theta^+)}$, $n_2 \gg 1$. This change can be computed numerically by summing the values of $\hat{\psi}$, with appropriate signs, at the vertices visited by the ray circuit. The total change can be written as

$$\left[n_2 + \Theta^+(\theta^+) - n_1 - \theta^+\right]\delta + \Delta^+(\theta^+), \tag{3.25}$$

where Δ^+ does not depend on n_1 or n_2 because to increment either by 1 adds a loop around the attractor at one end and changes $h(y)$ by $\mp\delta$ at that end. Owing to the reversibility of the ray circuit, $\Delta^+(\Theta^+(\theta^+)) = -\Delta^+(\theta^+)$.

Connecting the asymptotic forms, (3.20), of the solution at the two ends of the circuit, one finds

$$H^+(\Theta^+(\theta^+)) - H^+(\theta^+) = \Delta^+(\theta^+). \tag{3.26}$$

The general solution of this functional equation is

$$H^+(\theta^+) = -\tfrac{1}{2}\Delta^+(\theta^+) + J^+(\theta^+), \tag{3.27}$$

where J^+ is an arbitrary function satisfying the symmetry condition $J^+(\Theta^+(\theta^+)) = J^+(\theta^+)$. An analogous equation holds for the negative side of the attractor. There is insufficient information to determine the solution uniquely until the equations for H^+ and H^- can be linked through the dynamics in the inner region.

3.5. *The inner solution*

The inner solution is localized near the attractor and consists of four segments. I begin by defining coordinates parallel (ξ) and perpendicular (η) to the ray in each segment:

$$\left.\begin{array}{lll} \xi_1 = x, & \eta_1 = \epsilon^{-1}y & \text{(segment } OA\text{),} \\ \xi_2 = y, & \eta_2 = \epsilon^{-1}(x - X) & \text{(segment } AB\text{),} \\ \xi_3 = (X - x), & \eta_3 = \epsilon^{-1}(Y - y) & \text{(segment } BC\text{),} \\ \xi_4 = Y - y, & \eta_4 = \epsilon^{-1}(-x) & \text{(segment } CO\text{).} \end{array}\right\} \tag{3.28}$$

In segment j the parallel coordinate ξ_j runs from 0 to Ξ_j, where $\Xi_1 = \Xi_3 = X$ and $\Xi_2 = \Xi_4 = Y$. The perpendicular coordinate η_j is stretched to resolve the inner region of width $O(\epsilon)$. In segment j, the asymptotic inner solution is of the form

$$\tilde{\psi} \sim \tilde{\psi}_j^{(in)}(\xi_j, \eta_j) \tag{3.29}$$

and satisfies the equation

$$i\frac{\partial^2 \tilde{\psi}_j^{(in)}}{\partial \xi_j \partial \eta_j} + \frac{\partial^4 \tilde{\psi}_j^{(in)}}{\partial \eta_j^4} = 0, \tag{3.30}$$

which follows from (3.9) under the assumed scalings.

Part of the difficulty in solving (3.30) consists of connecting the four segments. Boundary conditions apply in the corner regions where the segments meet and the wave is reflected. Where segment j overlaps with segment $j + 1$, the asymptotic solution consists simply of the linear superposition of $\tilde{\psi}_j^{(in)}$ and $\tilde{\psi}_{j+1}^{(in)}$, because (3.30) is linear and homogeneous. In the corner region, ξ_j and ξ_{j+1} are essentially constant while η_j and η_{j+1} vary by $O(1)$. Therefore the corner solution is of the form

$$\tilde{\psi} \sim \tilde{\psi}_j^{(in)}(\varXi_j, \eta_j) + \tilde{\psi}_{j+1}^{(in)}(0, \eta_{j+1}). \tag{3.31}$$

The location of the boundary is given by

$$\eta_{j+1} = t_j^{-1}\eta_j + O(\epsilon). \tag{3.32}$$

From the boundary condition $\tilde{\psi} = -\hat{\psi}$, one obtains the relation

$$\tilde{\psi}_{j+1}^{(in)}(0, t_j^{-1}\eta_j) = -\tilde{\psi}_j^{(in)}(\varXi_j, \eta_j) - \hat{\psi}_j, \tag{3.33}$$

which connects the solutions in consecutive segments. (To satisfy the second boundary condition $\boldsymbol{n} \cdot \nabla \psi = 0$, a thinner boundary layer must intervene in the corner.) At the vertex O, the corresponding relation is

$$\tilde{\psi}_1^{(in)}(0, t_4^{-1}\eta_4) = -\tilde{\psi}_4^{(in)}(\varXi_4, \eta_4) - \hat{\psi}_4. \tag{3.34}$$

I now define a connected inner solution by concatenating the solutions in the various segments. To connect the perpendicular coordinates smoothly, let

$$\eta = \begin{cases} \eta_1 & \text{in segment } OA, \\ t_1\eta_2 & \text{in segment } AB, \\ t_1t_2\eta_3 & \text{in segment } BC, \\ t_1t_2t_3\eta_4 & \text{in segment } CO, \end{cases} \tag{3.35}$$

i.e. $\eta = f_j\eta_j$ in segment j, with $f_1 = 1$ and

$$f_j = \prod_{k=1}^{j-1} t_k \qquad (j > 1). \tag{3.36}$$

To leave (3.30) in the same form, the parallel coordinate ξ_j must be rescaled by a factor f_j^3. For a continuous concatenation of the parallel coordinates, let

$$\xi = \begin{cases} \xi_1 & \text{in segment } OA, \\ f_2^3\xi_2 + \varXi_1 & \text{in segment } AB, \\ f_3^3\xi_3 + \varXi_1 + f_2^3\varXi_2 & \text{in segment } BC, \\ f_4^3\xi_4 + \varXi_1 + f_2^3\varXi_2 + f_3^3\varXi_3 & \text{in segment } CO, \end{cases} \tag{3.37}$$

i.e. $\xi = \xi_1$ in segment 1 and

$$\xi = f_j^3\xi_j + \sum_{k=1}^{j-1} f_k^3 \varXi_k \tag{3.38}$$

in segment $j > 1$. This coordinate runs from 0 to $\varXi$ around the attractor, where

$$\varXi = \sum_{j=1}^{4} f_j^3 \varXi_j = \left(1 + t_1^3 t_2^3\right) X + t_1^3 \left(1 + t_2^3 t_3^3\right) Y. \tag{3.39}$$

The solution itself, away from the corners, may then be written in the form

$$\tilde{\psi} \sim \tilde{\psi}^{(in)}(\xi, \eta) \tag{3.40}$$

with

$$\tilde{\psi}^{(in)}(\xi, \eta) = (-1)^{j-1} \tilde{\psi}_j^{(in)}(\xi_j, \eta_j) + \sum_{k=1}^{j-1} (-1)^k \hat{\psi}_k \tag{3.41}$$

in segment j. The boundary condition (3.33) then translates simply into the condition that $\tilde{\psi}^{(in)}(\xi, \eta)$ be continuous at each vertex. Meanwhile, (3.30) becomes simply

$$i \frac{\partial^2 \tilde{\psi}^{(in)}}{\partial \xi \partial \eta} + \frac{\partial^4 \tilde{\psi}^{(in)}}{\partial \eta^4} = 0. \tag{3.42}$$

This concatenation procedure effectively 'irons out' the corners in the attractor, allowing the solution to proceed continuously. It is important to note that the coordinates (ξ, η) cover the corner regions twice. As noted above, in the corner regions, the asymptotic solution is the sum of the solutions in the segments that meet there.

In fact, the boundary condition at vertex O is different because the perpendicular coordinate η undergoes a net focusing by a factor of α after one loop around the attractor. The boundary condition there is

$$\tilde{\psi}^{(in)}(\varXi, \alpha\eta) = \tilde{\psi}^{(in)}(0, \eta) + \delta. \tag{3.43}$$

To satisfy this condition requires a kind of self-similar viscous spreading of the shear layer to compensate for the geometrical focusing. Such a self-similar expansion occurs in the solutions of Moore & Saffman (1969) for detached shear layers in rotating fluids, which were used by Rieutord *et al.* (2001) in their analysis of inertial waves in a spherical annulus.

Define a similarity variable

$$\tau = \mu^{-1/3} \eta \tag{3.44}$$

where $\mu = \xi + c$ with c to be determined. For τ to map continuously at the vertex O we require

$$(\varXi + c)^{-1/3} \alpha\eta = c^{-1/3} \eta \tag{3.45}$$

and therefore

$$c = \frac{\varXi}{\alpha^3 - 1}. \tag{3.46}$$

One then writes

$$\tilde{\psi}^{(in)}(\xi, \eta) = \frac{\xi}{\varXi} \delta + \Psi(\mu, \tau) \tag{3.47}$$

to accommodate the net increase around the loop. Here, μ runs from c to $c + \varXi$ around the attractor. Equation (3.42) translates into

$$i \left(\frac{\partial}{\partial \mu} - \frac{\tau}{3\mu} \frac{\partial}{\partial \tau} \right) \left(\mu^{-1/3} \frac{\partial \Psi}{\partial \tau} \right) + \mu^{-4/3} \frac{\partial^4 \Psi}{\partial \tau^4} = 0 \tag{3.48}$$

and the boundary condition (3.43) requires simple continuity:

$$\Psi(\varXi + c, \tau) = \Psi(c, \tau). \tag{3.49}$$

Making the further transformation

$$\mu = c\,\mathrm{e}^{\lambda}, \tag{3.50}$$

where λ runs from 0 to $3 \ln \alpha$, one obtains

$$\mathrm{i}\frac{\partial^2 \Psi}{\partial \lambda \partial \tau} - \frac{\mathrm{i}}{3}\frac{\partial \Psi}{\partial \tau} - \frac{\mathrm{i}\tau}{3}\frac{\partial^2 \Psi}{\partial \tau^2} + \frac{\partial^4 \Psi}{\partial \tau^4} = 0. \tag{3.51}$$

The coordinate λ is now periodic and ignorable, so the solutions are found by separation of variables to be of the form

$$\Psi_n = \mathrm{e}^{\mathrm{i}k_n \lambda}\chi_n(\tau), \tag{3.52}$$

where $k_n = 2n\pi/(3\ln\alpha)$, $n \in \mathbf{Z}$ and χ_n satisfies the ordinary differential equation

$$-\left(k_n + \tfrac{1}{3}\mathrm{i}\right)\chi_n' - \tfrac{1}{3}\mathrm{i}\tau\chi_n'' + \chi_n'''' = 0. \tag{3.53}$$

Solutions that do not diverge superexponentially as $|\tau| \to \infty$ can be obtained by the Laplace transform method as in Moore & Saffman (1969), leading to the integral representation

$$\chi_n'(\tau) = \mathrm{i}\int_0^\infty \mathrm{e}^{-\mathrm{i}p\tau}\mathrm{e}^{-p^3}p^{-3\mathrm{i}k_n}\,\mathrm{d}p. \tag{3.54}$$

(These functions are related to Moore–Saffman functions of complex order and can be expressed in terms of generalized hypergeometric functions.) The asymptotic behaviour is

$$\chi_n'(\tau) \sim (-3\mathrm{i}k_n)!\,\mathrm{e}^{-(3/2)\pi k_n}\tau^{-1+3\mathrm{i}k_n} \qquad \text{as } \tau \to +\infty, \tag{3.55}$$

$$\chi_n'(\tau) \sim -(-3\mathrm{i}k_n)!\,\mathrm{e}^{(3/2)\pi k_n}|\tau|^{-1+3\mathrm{i}k_n} \qquad \text{as } \tau \to -\infty. \tag{3.56}$$

Therefore, $\chi_0(\tau)$ diverges logarithmically as $\tau \to \pm\infty$, while $\chi_n(\tau)$ for $n \neq 0$ is bounded, but oscillates indefinitely. One may define $\chi_n(\tau)$ uniquely such that $\chi_n(0) = 0$, say. Then

$$\chi_n(\tau) \sim \frac{(-3\mathrm{i}k_n)!}{3\mathrm{i}k_n}\mathrm{e}^{\mp(3/2)\pi k_n}|\tau|^{3\mathrm{i}k_n} + c_n^{\pm} \qquad \text{as } \tau \to \pm\infty \tag{3.57}$$

for some constants $c_n^{\pm}$. In the case $n = 0$, however,

$$\chi_0(\tau) \sim \ln|\tau| + c_0^{\pm} \qquad \text{as } \tau \to \pm\infty. \tag{3.58}$$

The general solution of the inner problem is therefore given by (3.47) with

$$\Psi(\mu, \tau) = \sum_{n=-\infty}^{\infty} \mu^{\mathrm{i}k_n}\left[a_n\chi_n(\tau) + b_n\right], \tag{3.59}$$

where a_n and b_n are undetermined coefficients. Noting that $|\tau|^3\mu = |\eta|^3$ one finds the outer limit of the inner solution to be

$$\tilde{\psi}^{(in)}(\xi, \eta) \sim \frac{\xi}{\varXi}\delta + a_0\ln|\eta| - \tfrac{1}{3}a_0\ln(\xi + c) + a_0 c_0^{\pm} + b_0$$
$$+ \sum_{n\neq 0}\left[a_n\frac{(-3\mathrm{i}k_n)!}{3\mathrm{i}k_n}\mathrm{e}^{\mp(3/2)\pi k_n}|\eta|^{3\mathrm{i}k_n} + (a_n c_n^{\pm} + b_n)(\xi + c)^{\mathrm{i}k_n}\right] \tag{3.60}$$

as $\eta \to \pm\infty$.

3.6. Asymptotic matching

The aim is now to determine the coefficients a_n by matching the outer limit of the inner solution to the inner limit of the outer solution. (The coefficients b_n will not be required for a calculation of the asymptotic dissipation rate.) I consider the matching on segment 1; it is straightforward to show that the solution then matches in the same way on the other segments.

The inner limit of the outer solution near segment 1 is, for $y > 0$ or $y < 0$, respectively,

$$\psi^{(out)}(x, y) \sim g(0) - \left(-\frac{\ln|y|}{\ln\alpha}\right)\delta - H^{\pm}(\theta^{\pm}), \tag{3.61}$$

where again

$$\theta^{\pm} = \left(-\frac{\ln|y|}{\ln\alpha}\right) \bmod 1. \tag{3.62}$$

To compare this solution with the outer limit of the inner solution, (3.60), note that $\eta = \epsilon^{-1}y$ and therefore

$$|\eta|^{3ik_n} = e^{2n\pi i \ln|\eta|/\ln\alpha} = e^{-2n\pi i\theta^{\pm}}e^{-2n\pi i \ln\epsilon/\ln\alpha}. \tag{3.63}$$

I consider first the positive side $y > 0$ of the attractor and identify

$$a_0 = \frac{\delta}{\ln\alpha}, \tag{3.64}$$

$$a_n = -\frac{3ik_n}{(-3ik_n)!}e^{(3/2)\pi k_n}e^{2n\pi i \ln\epsilon/\ln\alpha}H^{+}_{-n} \qquad (n \neq 0). \tag{3.65}$$

Matching on the negative side yields the same expression for a_0, and

$$a_n = -\frac{3ik_n}{(-3ik_n)!}e^{-(3/2)\pi k_n}e^{2n\pi i \ln\epsilon/\ln\alpha}H^{-}_{-n} \qquad (n \neq 0). \tag{3.66}$$

It follows that the functions $H^{+}(\theta^{+})$ and $H^{-}(\theta^{-})$ are related to each other in the Fourier domain by

$$H^{+}_n = e^{3\pi k_n}H^{-}_n, \qquad n \neq 0. \tag{3.67}$$

(The mean values of $H^{\pm}$, $H^{\pm}_0$, are not determined by the matching procedure. The relation (3.67) implies that, if $H^{\pm}$ are analytic functions, they are identical except that their arguments are shifted by $i\pi/\ln\alpha$ in the complex plane and they also differ in value by an additive constant.) Physically, this relation is achieved by a viscous diffusion across the shear layer, which allows information to be transmitted across the characteristics of the inviscid equation.

Now using the identity

$$|(ix)!|^2 = \frac{\pi x}{\sinh(\pi x)} \tag{3.68}$$

for real x, one obtains

$$|a_{-n}|^2 = \frac{3k_n}{2\pi}(|H^{+}_n|^2 - |H^{-}_n|^2) \qquad (n \neq 0). \tag{3.69}$$

3.7. The dissipation rate

The energy dissipation rate D is of order unity in the limit $\epsilon \to 0$ and is dominated by the inner region. To see this, consider the following order-of-magnitude estimates, bearing in mind that the dissipation rate is the area integral of the viscosity multiplied

by the square of the vorticity. In the outer region, the streamfunction, velocity and vorticity are all $O(1)$, the area of the region is $O(1)$ and the dissipation rate is therefore $O(\epsilon^3)$; it is small just because the viscosity is small. In the boundary layers, the velocity is $O(1)$, the vorticity is $O(\epsilon^{-3/2})$, the area is $O(\epsilon^{3/2})$ and the dissipation rate is therefore $O(\epsilon^{3/2})$. Finally, in the inner region, the streamfunction is $O(1)$, the velocity is $O(\epsilon^{-1})$, the vorticity is $O(\epsilon^{-2})$, the area is $O(\epsilon)$ and the dissipation rate is therefore $O(1)$. I now calculate an exact asymptotic expression for the dissipation rate.

The element of area in segment j of the inner region is

$$\mathrm{d}A = \mathrm{d}x\,\mathrm{d}y = \epsilon\,\mathrm{d}\xi_j\,\mathrm{d}\eta_j = \epsilon f_j^{-4}\,\mathrm{d}\xi\,\mathrm{d}\eta. \tag{3.70}$$

Under the transformation from (ξ, η) to (μ, τ) this becomes

$$\mathrm{d}A = \epsilon f_j^{-4}\mu^{1/3}\,\mathrm{d}\mu\,\mathrm{d}\tau. \tag{3.71}$$

The vorticity is dominated by perpendicular derivatives of the streamfunction:

$$\nabla^2\psi \sim \epsilon^{-2}\frac{\partial^2\tilde{\psi}^{(in)}}{\partial\eta_j^2} = \epsilon^{-2}f_j^2\mu^{-2/3}\frac{\partial^2\Psi}{\partial\tau^2}. \tag{3.72}$$

The dissipation rate at leading order therefore simplifies to

$$D \sim \tfrac{1}{2}\int_{-\infty}^{\infty}\int_0^{3\ln\alpha}\left|\frac{\partial^2\Psi}{\partial\tau^2}\right|^2\,\mathrm{d}\lambda\,\mathrm{d}\tau. \tag{3.73}$$

The different 'modes' proportional to $\mathrm{e}^{\mathrm{i}k_n\lambda}$ add in quadrature with the result

$$D \sim \tfrac{3}{2}\ln\alpha\sum_{n=-\infty}^{\infty}|a_n|^2 d_n, \tag{3.74}$$

where

$$d_n = \int_{-\infty}^{\infty}|\chi_n''(\tau)|^2\,\mathrm{d}\tau \tag{3.75}$$

is merely a property of the basis functions. The integrals d_n are convergent; the dissipation is well localized even if the streamfunction is not. To evaluate d_n, I use the integral representation (3.54) to obtain

$$d_n = \int_{-\infty}^{\infty}\int_0^{\infty}\int_0^{\infty}\mathrm{e}^{\mathrm{i}(q-p)\tau}\mathrm{e}^{-p^3-q^3}\left(\frac{q}{p}\right)^{3\mathrm{i}k_n}pq\,\mathrm{d}p\,\mathrm{d}q\,\mathrm{d}\tau. \tag{3.76}$$

The integration with respect to τ is carried out first, using the identity

$$\int_{-\infty}^{\infty}\mathrm{e}^{\mathrm{i}(q-p)\tau}\,\mathrm{d}\tau = 2\pi\delta(q-p), \tag{3.77}$$

and leading to the simple result

$$d_n = 2\pi\int_0^{\infty}\mathrm{e}^{-2p^3}p^2\,\mathrm{d}p = \tfrac{1}{3}\pi. \tag{3.78}$$

The asymptotic dissipation rate is therefore

$$D \sim \tfrac{1}{2}\pi\ln\alpha\sum_{n=-\infty}^{\infty}|a_n|^2. \tag{3.79}$$

Note that $|a_n|^2$ can be related to the outer solution by (3.64) or (3.69).

4. A problem with a non-viscous damping force

4.1. *Motivation*

In this section, I investigate a related problem in which the weak viscous force, which depends on second derivatives of the velocity, is replaced by a weak damping force of non-viscous form, depending on the velocity itself. I show below that the same asymptotic dissipation rate is obtained in this case, implying that the dissipation rate is robust, being independent of both the magnitude and the form of the damping force in the limit that the damping is weak.

One reason for investigating this robustness is that the true mechanism by which tidal disturbances in astrophysical bodies, such as inertial waves in the convective regions of giant planets, are damped is uncertain. The true viscosity is exceedingly small, and the waves may decay more readily by other means. Their interaction with convective motions might be modelled in terms of an eddy viscosity, but the validity of such an approach is unclear and estimates of the relevant effective viscosity vary widely. Alternatively, inertial waves may undergo Ohmic damping in the presence of a magnetic field since they couple to Alfvén waves on small scales. They may also experience nonlinear parametric decay into waves of shorter wavelength. The last two mechanisms are probably modelled more accurately, although still only crudely, by using a 'frictional' damping force proportional to the velocity, rather than a viscous force.

Another way to view the following analysis is that it results from the Landau prescription in which the frequency of the forced wave is given a small positive imaginary part, thereby rendering the inviscid problem soluble, and a limit is taken in which the imaginary part of the frequency tends to zero. Such an approach might be justified by a consideration of the late-time asymptotic solution of the inviscid initial-value problem constructed by a Laplace transform method.

4.2. *Sketch of the analysis*

Instead of (3.1), I now consider

$$\mathrm{i}\frac{\partial^2 \psi}{\partial x \partial y} - \epsilon \nabla^2 \psi = f, \tag{4.1}$$

with the boundary condition

$$\psi = 0 \qquad \text{on } \partial \mathcal{D}. \tag{4.2}$$

The dissipation rate for this problem is

$$D = \tfrac{1}{2}\int_{\mathcal{D}} \epsilon |\nabla \psi|^2 \, \mathrm{d}A = \tfrac{1}{2}\mathrm{Re}\int_{\mathcal{D}} \psi^* f \, \mathrm{d}A. \tag{4.3}$$

The analysis proceeds in a very similar way to the previous calculation and it is necessary only to point out the essential differences. One simplification is that no viscous boundary layers occur, although, in fact, it was not necessary to consider the boundary layers of the previous problem in any detail. The essential differences appear in the analysis of the inner region, which is again of width $O(\epsilon)$. The reduced equation (3.30) in segment j becomes

$$\mathrm{i}\frac{\partial^2 \tilde{\psi}_j^{(in)}}{\partial \xi_j \partial \eta_j} - \frac{\partial^2 \tilde{\psi}_j^{(in)}}{\partial \eta_j^2} = 0. \tag{4.4}$$

The factors of f^3 and t^3 in (3.37)–(3.39) should be replaced by single powers and the concatenated inner equation (3.42) becomes

$$i\frac{\partial^2 \tilde{\psi}^{(in)}}{\partial \xi \partial \eta} - \frac{\partial^2 \tilde{\psi}^{(in)}}{\partial \eta^2} = 0. \tag{4.5}$$

A similarity solution satisfying the boundary conditions can be obtained in an analogous way, now using variables $\tau = \eta/(\xi + c)$ and $\lambda = \ln(\xi/c + 1)$ with $c = \Xi/(\alpha - 1)$. The parallel coordinate λ runs from 0 to $\ln \alpha$, not $3 \ln \alpha$ as previously. The inner equation in similarity variables now reads

$$i\frac{\partial^2 \Psi}{\partial \lambda \partial \tau} - i\frac{\partial \Psi}{\partial \tau} - i\tau \frac{\partial^2 \Psi}{\partial \tau^2} - \frac{\partial^2 \Psi}{\partial \tau^2} = 0 \tag{4.6}$$

and has solutions

$$\Psi_n = e^{3ik_n\lambda} \chi_n(\tau) \tag{4.7}$$

where I define $k_n = 2n\pi/(3 \ln \alpha)$ as previously, and χ_n now satisfies

$$-(3k_n + i)\chi'_n - i\tau \chi''_n - \chi''_n = 0. \tag{4.8}$$

The Laplace transform method leads to

$$\chi'_n(\tau) = i\int_0^\infty e^{-ip\tau} e^{-p} p^{-3ik_n} \, dp = (-3ik_n)! \, e^{-(3/2)\pi k_n} (\tau - i)^{-1+3ik_n}, \tag{4.9}$$

where the branch cut is confined to the upper half-plane. The asymptotic behaviour as $\tau \to \pm\infty$ is precisely as in (3.55) and (3.56), and the asymptotic matching therefore yields precisely the same values for the coefficients a_n.

Finally, the asymptotic dissipation rate is computed as

$$D \sim \frac{1}{2} \int_{-\infty}^\infty \int_0^{\ln \alpha} \left| \frac{\partial \Psi}{\partial \tau} \right|^2 \, d\lambda \, d\tau \sim \frac{1}{2} \ln \alpha \sum_{n=-\infty}^\infty |a_n|^2 d_n, \tag{4.10}$$

where now

$$d_n = \int_{-\infty}^\infty |\chi'_n(\tau)|^2 \, d\tau = \pi. \tag{4.11}$$

The end result is that the asymptotic dissipation rate is exactly the same as for the viscous problem,

$$D \sim \frac{1}{2}\pi \ln \alpha \sum_{n=-\infty}^\infty |a_n|^2. \tag{4.12}$$

5. Numerical solutions

Numerical solutions of (2.6), (3.1) and (4.1) in various quadrilateral domains have been obtained by the following method. A nonlinear algebraic coordinate transformation is first applied to map the quadrilateral domain onto the unit square. The equations are then discretized using centred second-order finite differences, resulting in a large linear system in block tridiagonal form. This is solved by a direct method and the total dissipation rate is evaluated, again to second-order accuracy, from a numerical integration based on either (2.9) or (2.10) (or their equivalents for the other differential equations). Typically, (2.10) gives a much more accurate numerical value for D, as it does not require a numerical differentiation of the solution.
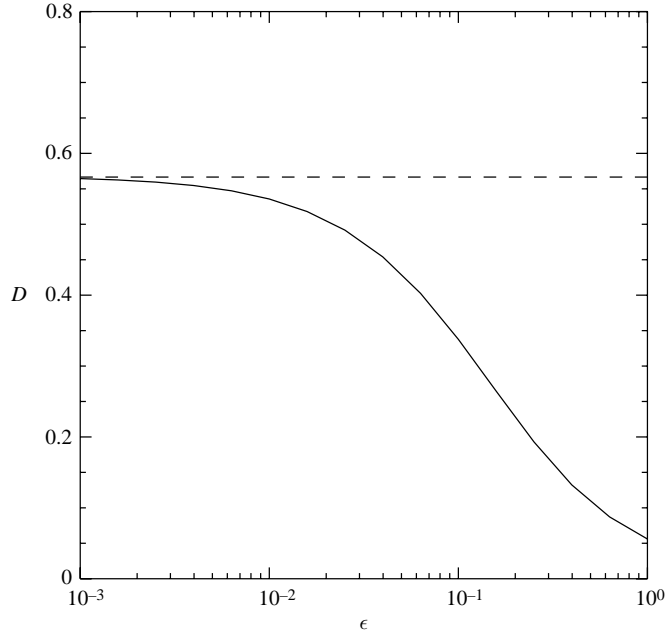
FIGURE 2. Dissipation rate versus damping parameter for (4.1) in a tilted square domain ($X = Y = 1$, $t_i = 2$) with uniform forcing ($f = 1$). The dashed line indicates the limiting value expected on the basis of the asymptotic analysis.
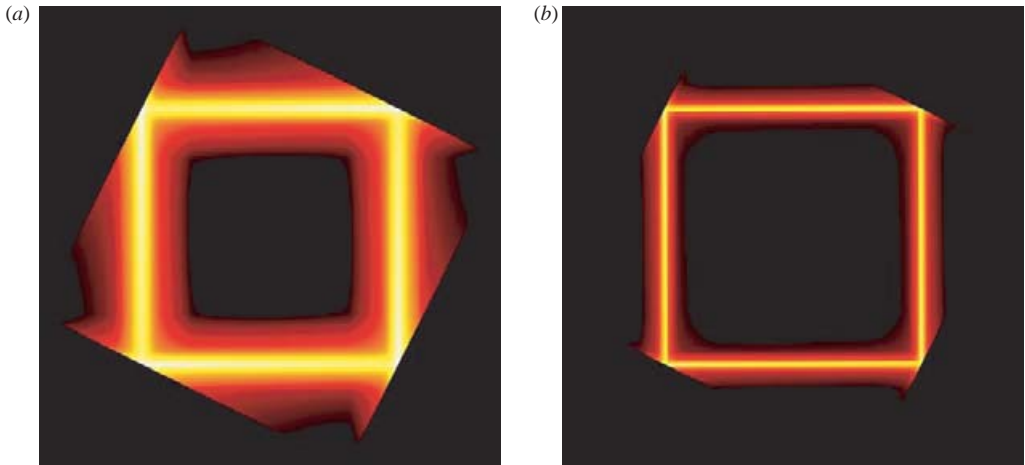

FIGURE 3. Spatial distribution of the dissipation rate for the problem referred to in figure 2. (*a*) $\epsilon = 0.01$ and (*b*) 0.003. In each case, a logarithmic colour scale over three orders of magnitude is used.

One of the simplest problems involving a wave attractor is to solve (4.1) in a tilted square domain ($X = Y = 1$, $t_1 = t_2 = t_3 = t_4 \neq 1$) with uniform forcing ($f = 1$). The dissipation rate for the case $t_i = 2$ is plotted as a function of ϵ in figure 2, showing the anticipated convergence to a non-zero limit as $\epsilon \to 0$. Of course, a higher numerical resolution is required when ϵ is reduced. Figure 3 shows the spatial distribution of the dissipation rate for $\epsilon = 0.01$ and 0.003 as calculated with a numerical resolution
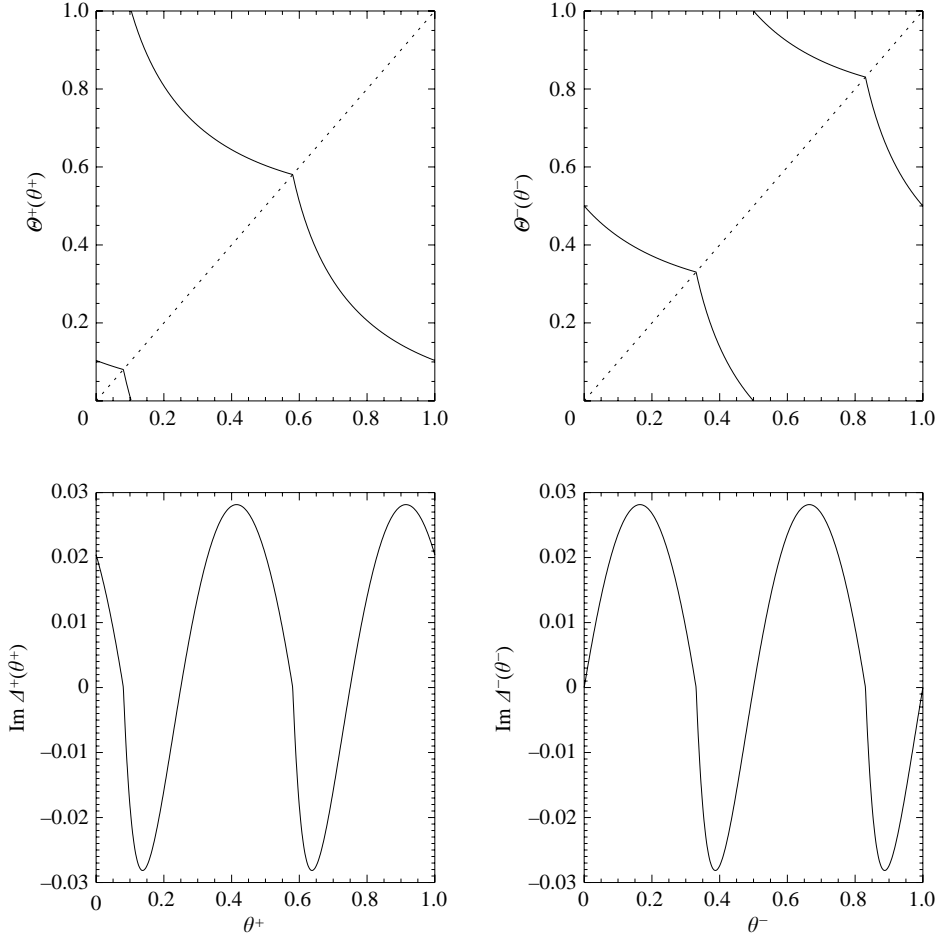
FIGURE 4. The ray-mapping and forcing functions in the tilted square domain
($X = Y = 1$, $t_i = 2$) with uniform forcing ($f = 1$).

of 1000^2. As expected from the asymptotic solution, the dissipation is localized in the neighbourhood of the attractor and the width of the beam is proportional to ϵ.

To determine the expected limiting value of D from the asymptotic analytical solution, some calculation is required. The focusing and forcing constants α and δ are easily evaluated. A simple program is then used to follow the propagation of rays in the quadrilateral domain and thereby to evaluate the ray-mapping and forcing functions $\Theta^\pm(\theta^\pm)$ and $\Delta^\pm(\theta^\pm)$; these are shown in figure 4.

Next the functional equations

$$H^\pm(\Theta^\pm(\theta^\pm)) - H^\pm(\theta^+) = \Delta^\pm(\theta^\pm) \tag{5.1}$$

must be solved, subject to the coupling condition on the Fourier coefficients

$$H_n^+ = e^{3\pi k_n} H_n^- \qquad (n \neq 0). \tag{5.2}$$

Equations (5.1) can be represented in the Fourier domain in the form

$$\sum_{n=-\infty}^{\infty} M_{mn}^\pm H_n^\pm - H_m^\pm = \Delta_m^\pm, \tag{5.3}$$

where

$$M_{mn}^{\pm} = \int_0^1 e^{-2m\pi i\theta^{\pm}} e^{2n\pi i\Theta^{\pm}(\theta^{\pm})} \, d\theta^{\pm}, \tag{5.4}$$

$$\Delta_m^{\pm} = \int_0^1 e^{-2m\pi i\theta^{\pm}} \Delta^{\pm}(\theta^{\pm}) \, d\theta^{\pm}. \tag{5.5}$$

Equations (5.3) are semi-redundant because the symmetry properties $\Theta^{\pm}(\Theta^{\pm}(\theta^{\pm})) = \theta^{\pm}$ and $\Delta^{\pm}(\Theta^{\pm}(\theta^{\pm})) = -\Delta^{\pm}(\theta^{\pm})$ ensure that the equations merely change sign when acted upon by the appropriate operator with matrix coefficients $M_{mn}^{\pm}$. It is most convenient, for numerical purposes, to regard the unknown quantities as the 'large' Fourier coefficients H_n^+ ($1 \leqslant n \leqslant N$) and H_n^- ($-N \leqslant n \leqslant -1$) up to some finite truncation order N, substituting for the 'small' coefficients using (5.2). The property $M_{m0}^{\pm} = \delta_{m0}$ means that the quantities $H_0^{\pm}$ cannot be determined and in any case are not required in order to calculate the asymptotic dissipation rate. In view of the semi-redundancy, it is sufficient to solve only half of the truncated system of (5.3), e.g. the '+' equations for $m > 0$ and the '−' equations for $m < 0$. The coefficients $M_{mn}^{\pm}$ and $\Delta_m^{\pm}$ are readily calculated to high accuracy from the computed functions $\Theta^{\pm}(\theta^{\pm})$ and $\Delta^{\pm}(\theta^{\pm})$.

In practice, it is found that, for a smooth forcing function f, the coefficients a_n typically decay rapidly with n so that a_0 makes by far the dominant contribution to D. This property is very convenient because a_0 is easily calculated and does not depend on the details of the global ray mapping. The dashed line in figure 2 indicates the expected asymptotic value of D, to which terms other than a_0 contribute less than 1%. Convergence to the same dissipation rate is found for the viscous problem defined by (3.1).

The asymptotic analytical solution is compared in detail with the direct numerical solution in figure 5, which shows the y-component of the velocity along a cross-section through the tilted square domain at $y = 0.3$. In drawing the asymptotic solution along this section, the inner solutions corresponding to segments 2 and 4 are summed. No attempt is made to patch with the outer solution, which is much smaller and more difficult to determine properly. Even with this restriction the agreement is very good at $\epsilon = 0.01$.

6. Discussion

In this paper, I have considered a prototypical forced linear wave equation featuring a wave attractor and weak viscous damping. This mathematical problem describes the long-term linear response of a typical bounded fluid to a periodic body force with a frequency within the range of inertial and gravity waves. Through asymptotic analysis confirmed by direct numerical calculations in an illustrative quadrilateral domain, I have shown that the forced disturbance is localized in the neighbourhood of the attractor and that the total dissipation rate is asymptotically independent of the viscosity. By considering a related equation with a non-viscous damping force, I have argued further that the asymptotic dissipation rate is independent of the nature, as well as the magnitude, of the weak damping mechanism.

These findings have important consequences for physical problems such as that considered in §2 and motivated by the experiments of Maas *et al.* (1997), in which a periodic body force excites internal gravity waves in a narrow tank of non-rectangular cross-section. In that problem, the wave attractors exist in certain intervals of frequency that depend only on the geometry of the container. The long-term linear
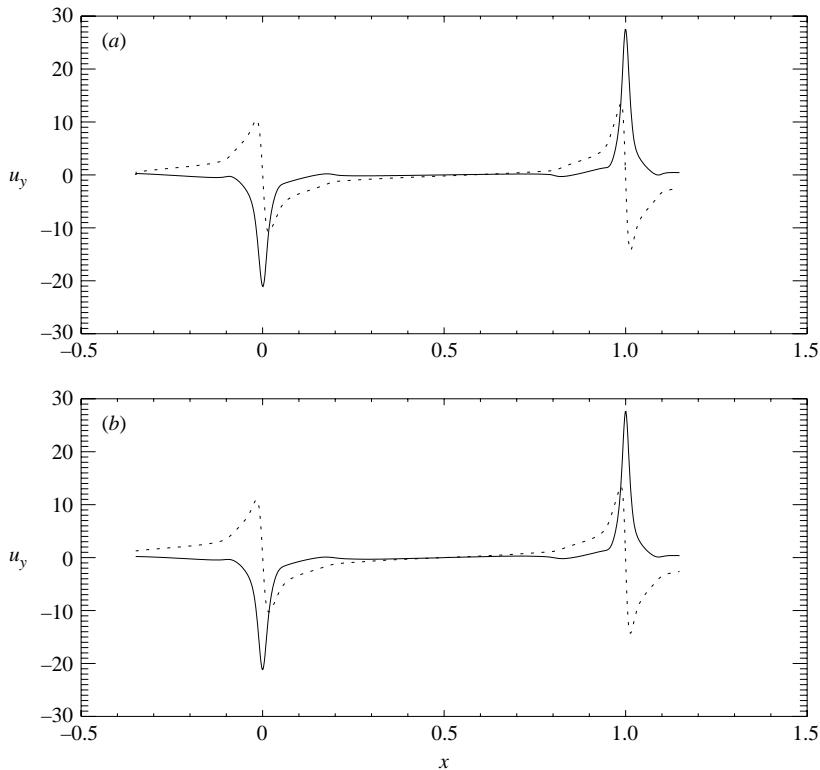
FIGURE 5. Cross-section at height $y = 0.3$ of the y-component of velocity, defined by $u_y = -\partial\psi/\partial x$, for the problem referred to in figure 2 with $\epsilon = 0.01$. (a) The direct numerical solution, (b) the sum of the asymptotic inner solutions for segments 2 and 4. —, real and ..., imaginary parts of u_y.

response of the fluid should give rise to a dissipation rate that is asymptotically independent of the viscosity and is a smoothly varying function of the forcing frequency within the interval associated with a given attractor. This differs markedly from the case of an upright rectangular tank, in which the response of the fluid is governed by resonances with the regular inviscid normal modes that can exist in that container, and the dissipation rate will be very small except where it is strongly amplified in the vicinity of the resonant frequencies of the lowest-order modes. As noted by Maas *et al.* (1997), wave attractors have a 'finite bandwidth' while the width of a normal-mode resonance is limited by viscosity.

Ogilvie & Lin (2004) studied the linear response of a giant planet with an extended convective region to periodic tidal forcing. Inertial waves propagating in the annular convective region do not form regular eigenfunctions in the absence of viscosity. Numerical solutions indicated that, when the Ekman number is small, the disturbance tends to be localized on a web of rays. For intervals of frequency in which simple wave attractors exist, it was possible to identify their appearance in the solutions. In figure 10 of Ogilvie & Lin (2004) it can be seen that the dissipation rate appears to have converged to a value independent of the viscosity in the intervals where the dissipation rate is largest. It can be confirmed by tracing rays in the annulus that these intervals are those associated with the simplest and most powerfully focusing wave attractors. Although more complicated attractors exist outside these intervals,

their focusing power is evidently not great enough to have led to a convergence of the dissipation rate at an Ekman number of 10^{-8}. These numerical results are qualitatively consistent with the conclusions of the present paper, and in future work we will attempt to evaluate the asymptotic dissipation rate for tidal forcing in a spherical annulus directly using the methods described here.

Forced inertial waves in a rotating incompressible fluid contained in a spherical annulus were computed by Tilgner (1999), who noted that wave attractors can be detected in the solutions at small Ekman numbers, but that other complicating features are also present. In his problem, which derives from earlier experimental studies, the forcing results from a sinusoidal modulation of the rotation rate of the boundaries, which is communicated to the fluid through viscous boundary layers. As the viscosity is reduced, the energy of the forced disturbance is also diminished. This behaviour is different from that found in the present paper with a distributed body force that is independent of viscosity, such as that resulting from tidal forcing.

The apparent robustness of the dissipation rate is reassuring when it is considered that the true mechanism by which the inertial waves are damped is uncertain and difficult to model accurately. It is likely that the result is reasonably robust in other ways as well. For example, small corrugations of the boundary may not be as important for inertial waves as for acoustic waves, which undergo specular reflection. Inertial waves of a given frequency can propagate only in four different directions, and the angle of reflection will not be changed by a small corrugation. The wave attractors depend more on the gross shape of the container than on the precise contours of the boundary.

It is also noteworthy that the 'inner' equations (3.30) and (4.4) studied in this paper are generic in the following sense. Provided that the inviscid wave equation is a hyperbolic second-order linear partial differential equation, its characteristics can be determined and any wave attractors identified. Curvilinear coordinates can then be introduced parallel and perpendicular to each segment of the attractor. If the equation contains a weak damping term resulting from a positive operator of either fourth or second order, then the coordinates can always be rescaled to obtain (3.30) or (4.4), respectively. This is true even if the inviscid equation has non-constant coefficients and the damping operator is anisotropic and depends on position, provided that there are no singularities such as corotation resonances or critical latitudes.

Further work is required to understand the transition from normal modes to wave attractors as the geometry of the container is varied. Ogilvie & Lin (2004) found that some 'memory' of the normal modes of inertial waves in a full sphere was retained when a small solid core was introduced. Even though no inviscid normal modes are believed to exist in a spherical annulus, the dissipation rate is still enhanced in the vicinity of the eigenfrequencies of the lowest-order modes of the full sphere. An imperfect resonance is possible with such modes, which have a length-scale larger than the radius of the core and are not greatly affected by it. At the same time, introduction of the solid core allows a much richer response at other frequencies, associated with wave attractors. It is possible that in such problems the attractors achieve complete dominance only at Ekman numbers yet smaller than those achieved in recent numerical studies.

A remarkable theory of axisymmetric inertial waves in an incompressible rotating fluid contained in a spherical annulus was developed by Rieutord *et al.* (2002), who considered normal modes that are regularized and damped by viscosity. Their problem is similar to that considered in the present paper, but there are also important differences. Neglecting some of the effects of curvature so as to make the equations

somewhat simpler, they found asymptotic solutions for normal modes in the limit of small Ekman number, in excellent agreement with their numerical calculations. The modes are localized near a wave attractor and satisfy an eigenvalue problem analogous to that for the wavefunction of a quantum-mechanical harmonic oscillator. The width of the shear layers in these modes scales with $\nu^{1/4}$, although the authors noted that $\nu^{1/3}$ layers also play a role when the problem is studied in full spherical geometry. In contrast, the solutions described in §3 have only a $\nu^{1/3}$ shear layer and satisfy a different inner equation that has no strictly localized solutions but is forced from the outside. The reason for the different scalings is that the normal modes considered by Rieutord *et al.* (2002) have frequencies that are asymptotically close to the edge of the band within which the attractor exists, so that the attractor is very weak and its focusing power α is asymptotically close to 1. In contrast, the forced solutions in the present paper are constructed for the more interesting frequencies that lie properly within the bandwidth of the attractor, so that α is not very close to 1. It is likely that a different asymptotic theory of forced oscillations could be constructed for values of α very close to 1, which would more closely resemble the analysis of Rieutord *et al.* (2002). However, it still remains to be demonstrated in detail how the analysis in the present paper applies to forced oscillations in spherical geometry.

Appendix A. Character of the inviscid linearized equations

The equations governing the dynamics of an ideal fluid with negligible self-gravity may be written

$$\frac{\mathrm{D}\boldsymbol{u}}{\mathrm{D}t} = -\frac{1}{\rho}\nabla p - \nabla\Phi, \tag{A 1}$$

$$\frac{\mathrm{D}\rho}{\mathrm{D}t} = -\rho\nabla \cdot \boldsymbol{u}, \tag{A 2}$$

$$\frac{\mathrm{D}p}{\mathrm{D}t} = -\gamma p\nabla \cdot \boldsymbol{u}, \tag{A 3}$$

where Φ is the external gravitational potential and the notation is standard. Let (r, ϕ, z) be cylindrical polar coordinates and consider a basic state consisting of an axisymmetric fluid body with angular velocity $\Omega(r, z)$ and no meridional flow. For small perturbations of the form

$$\mathrm{Re}\left[\boldsymbol{u}'(r, z)\,\mathrm{e}^{-\mathrm{i}\omega t + \mathrm{i}m\phi}\right], \tag{A 4}$$

etc., the linearized equations read

$$-\mathrm{i}\hat{\omega}u_r' - 2\Omega u_\phi' = -\frac{1}{\rho}\frac{\partial p'}{\partial r} + \frac{\rho'}{\rho^2}\frac{\partial p}{\partial r}, \tag{A 5}$$

$$-\mathrm{i}\hat{\omega}u_\phi' + \frac{1}{r}\left(u_r'\frac{\partial}{\partial r} + u_z'\frac{\partial}{\partial z}\right)(r^2\Omega) = -\frac{\mathrm{i}mp'}{\rho r}, \tag{A 6}$$

$$-i\hat{\omega}u_z' = -\frac{1}{\rho}\frac{\partial p'}{\partial z} + \frac{\rho'}{\rho^2}\frac{\partial p}{\partial z}, \tag{A 7}$$

$$-i\hat{\omega}\rho' + u_r'\frac{\partial \rho}{\partial r} + u_z'\frac{\partial \rho}{\partial z} = -\rho\left[\frac{1}{r}\frac{\partial}{\partial r}(ru_r') + \frac{imu_\phi'}{r} + \frac{\partial u_z'}{\partial z}\right], \tag{A 8}$$

$$-i\hat{\omega}p' + u_r'\frac{\partial p}{\partial r} + u_z'\frac{\partial p}{\partial z} = -\gamma p\left[\frac{1}{r}\frac{\partial}{\partial r}(ru_r') + \frac{imu_\phi'}{r} + \frac{\partial u_z'}{\partial z}\right], \tag{A 9}$$

where $\hat{\omega} = \omega - m\Omega$ is the Doppler-shifted wave frequency. Eliminate u_ϕ' and ρ' to obtain

$$(\hat{\omega}^2 - A)u_r' - Bu_z' = -\frac{i\hat{\omega}}{\rho}\left(\frac{\partial p'}{\partial r} - \frac{\partial p}{\partial r}\frac{p'}{\gamma p}\right) + 2\Omega\frac{imp'}{\rho r}, \tag{A 10}$$

$$-Cu_r' + (\hat{\omega}^2 - D)u_z' = -\frac{i\hat{\omega}}{\rho}\left(\frac{\partial p'}{\partial z} - \frac{\partial p}{\partial z}\frac{p'}{\gamma p}\right), \tag{A 11}$$

where

$$A = \frac{2\Omega}{r}\frac{\partial}{\partial r}(r^2\Omega) - \frac{1}{\rho}\frac{\partial p}{\partial r}\left(\frac{1}{\gamma p}\frac{\partial p}{\partial r} - \frac{1}{\rho}\frac{\partial \rho}{\partial r}\right), \tag{A 12}$$

$$B = \frac{2\Omega}{r}\frac{\partial}{\partial z}(r^2\Omega) - \frac{1}{\rho}\frac{\partial p}{\partial r}\left(\frac{1}{\gamma p}\frac{\partial p}{\partial z} - \frac{1}{\rho}\frac{\partial \rho}{\partial z}\right), \tag{A 13}$$

$$C = -\frac{1}{\rho}\frac{\partial p}{\partial z}\left(\frac{1}{\gamma p}\frac{\partial p}{\partial r} - \frac{1}{\rho}\frac{\partial \rho}{\partial r}\right), \tag{A 14}$$

$$D = -\frac{1}{\rho}\frac{\partial p}{\partial z}\left(\frac{1}{\gamma p}\frac{\partial p}{\partial z} - \frac{1}{\rho}\frac{\partial \rho}{\partial z}\right). \tag{A 15}$$

Then eliminate u_r' and u_z' to obtain

$$(\hat{\omega}^2 - D)\frac{\partial^2 p'}{\partial r^2} + (B + C)\frac{\partial^2 p'}{\partial r\partial z} + (\hat{\omega}^2 - A)\frac{\partial^2 p'}{\partial z^2} + (\text{terms in } p' \text{ and } \nabla p') = 0. \tag{A 16}$$

This equation is hyperbolic when

$$4(\hat{\omega}^2 - A)(\hat{\omega}^2 - D) < (B + C)^2, \tag{A 17}$$

i.e. for frequencies such that

$$(A + D)^2 - [(B + C)^2 + (A - D)^2]^{1/2} < 2\hat{\omega}^2 < (A + D)^2 + [(B + C)^2 + (A - D)^2]^{1/2}. \tag{A 18}$$

(The Høiland criteria for stability with respect to axisymmetric perturbations are $A + D > 0$ and $AD > BC$ (e.g. Tassoul 1978). For a Høiland-stable basic state the hyperbolic range of frequencies may or may not include $\hat{\omega} = 0$.)

Appendix B. Vortical effective forcing

Ogilvie & Lin (2004) studied the linear response of a rotating giant planet (or star) to tidal forcing in circumstances in which the forcing frequency is comparable to the angular velocity Ω of the body, but small compared to its dynamical frequency $(GM/R^3)^{1/2}$. They used a consistent asymptotic expansion to simplify the equations satisfied by the tidal disturbance in both convective and radiative regions. The tidal

force, which derives from a perturbing gravitational potential, is taken up by a quasi-hydrostatic adjustment (a tidal bulge) known as the equilibrium tide. Because the tidal frequency is non-zero, the motion of the bulge gives rise to a non-zero velocity field $\boldsymbol{u}_e$ associated with the equilibrium tide, which can be derived analytically. The existence of inertial forces associated with this flow mean that the quasi-hydrostatic bulge does not quite satisfy the equation of motion and a residual force appears.

In quantitative terms, the total velocity perturbation $\boldsymbol{u}$ in an adiabatically stratified (i.e. convective) region satisfies the equations

$$-\mathrm{i}\hat{\omega}\boldsymbol{u} + 2\Omega \times \boldsymbol{u} = -\nabla W, \tag{B 1}$$

$$\frac{\partial \rho'_e}{\partial t} + \nabla \cdot (\rho \boldsymbol{u}) = 0, \tag{B 2}$$

where $\hat{\omega} = \omega - m\Omega$ is the Doppler-shifted frequency as in Appendix A, W is the pressure perturbation divided by the density, plus the total gravitational potential perturbation, and ρ'_e is the density perturbation associated with the equilibrium tide (any additional density perturbation being much smaller). Here it is assumed for simplicity that the fluid is uniformly rotating and the viscosity is neglected. Now since

$$\frac{\partial \rho'_e}{\partial t} + \nabla \cdot (\rho \boldsymbol{u}_e) = 0, \tag{B 3}$$

the residual 'dynamical tide' $\boldsymbol{u}_d = \boldsymbol{u} - \boldsymbol{u}_e$ is found to satisfy the equations

$$-\mathrm{i}\hat{\omega}\boldsymbol{u}_d + 2\Omega \times \boldsymbol{u}_d = -\nabla W + \boldsymbol{a}, \tag{B 4}$$

$$\nabla \cdot (\rho \boldsymbol{u}_d) = 0, \tag{B 5}$$

where

$$\boldsymbol{a} = \mathrm{i}\hat{\omega}\boldsymbol{u}_e - 2\Omega \times \boldsymbol{u}_e. \tag{B 6}$$

The dynamical tide therefore obeys the anelastic approximation, in which the modified pressure perturbation W must adjust to satisfy the constraint $\nabla \cdot (\rho \boldsymbol{u}_d) = 0$, and is driven by an effective body force $\boldsymbol{a}$ per unit mass. In general, this effective force is vortical, because $\nabla \times \boldsymbol{a} \neq \boldsymbol{0}$.

REFERENCES

ALDRIDGE, K. D. & LUMB, L. I. 1987 Inertial waves identified in the Earth's fluid outer core. *Nature* **325**, 421–423.

BRETHERTON, F. P. 1964 Low-frequency oscillations trapped near the equator. *Tellus* **16**, 181–185.

CHANDRASEKHAR, S. 1961 *Hydrodynamic and Hydromagnetic Stability.* Oxford University Press.

CHRISTENSEN-DALSGAARD, J. 2002 Helioseismology. *Rev. Mod. Phys.* **74**, 1073–1129.

GOLDREICH, P. & TREMAINE, S. 1980 Disk–satellite interactions. *Astrophys. J.* **241**, 425–441.

GREENSPAN, H. P. 1968 *The Theory of Rotating Fluids.* Cambridge University Press.

HOLLERBACH, R. & KERSWELL, R. R. 1995 Oscillatory internal shear layers in rotating and precessing flows. *J. Fluid Mech.* **298**, 327–339.

IOANNOU, P. J. & LINDZEN, R. S. 1993 Gravitational tides in the outer planets. I. Implications of classical tidal theory. *Astrophys. J.* **406**, 252–265.

KATO, S. 2001 Basic properties of thin-disk oscillations. *Proc. Astr. Soc. Japan* **53**, 1–24.

MAAS, L. R. M. 2001 Wave focusing and ensuing mean flow due to symmetry breaking in rotating fluids. *J. Fluid Mech.* **437**, 13–28.

MAAS, L. R. M., BENIELLI, D., SOMMERIA, J. & LAM, F.-P. A. 1997 Observation of an internal wave attractor in a confined, stably stratified fluid. *Nature* **388**, 557–561.

MAAS, L. R. M. & LAM, F.-P. A. 1995 Geometric focusing of internal waves. *J. Fluid Mech.* **300**, 1–41.

MANDERS, A. M. M. & MAAS, L. R. M. 2003 Observations of inertial waves in a rectangular basin with one sloping boundary. *J. Fluid Mech.* **493**, 59–88.

MOORE, D. W. & SAFFMAN, P. G. 1969 The structure of free vertical shear layers in a rotating fluid and the motion produced by a slowly rising body. *Phil. Trans. R. Soc. Lond.* A **264**, 597–634.

OGILVIE, G. I. & LIN, D. N. C. 2004 Tidal dissipation in rotating giant planets. *Astrophys. J.* **610**, 477–509.

RIEUTORD, M., GEORGEOT, B. & VALDETTARO, L. 2001 Inertial waves in a rotating spherical shell: attractors and asymptotic spectrum. *J. Fluid Mech.* **435**, 103–144.

RIEUTORD, M. & VALDETTARO, L. 1997 Inertial waves in a rotating spherical shell. *J. Fluid Mech.* **341**, 77–99.

RIEUTORD, M., VALDETTARO, L. & GEORGEOT, B. 2002 Analysis of singular inertial modes in a spherical shell: the slender toroidal shell model. *J. Fluid Mech.* **463**, 345–360.

SAVONIJE, G. J. & PAPALOIZOU, J. C. B. 1997 Non-adiabatic tidal forcing of a massive, uniformly rotating star – II. The low-frequency, inertial regime. *Mon. Not. R. Astr. Soc.* **291**, 633–650.

SAVONIJE, G. J., PAPALOIZOU, J. C. B. & ALBERTS, F. 1995 Non-adiabatic tidal forcing of a massive, uniformly rotating star. *Mon. Not. R. Astr. Soc.* **277**, 471–496.

SAVONIJE, G. J. & WITTE, M. G. 2002 Tidal interaction of a rotating 1 $M_\odot$ star with a binary companion. *Astr. Astrophys.* **386**, 211–221.

STERN, M. E. 1963 Trapping of low-frequency oscillations in an equatorial 'boundary layer'. *Tellus* **15**, 246–250.

STEWARTSON, K. 1972 On trapped oscillations in a slightly viscous rotating fluid. *J. Fluid Mech.* **54**, 749–761.

STEWARTSON, K. & RICKARD, J. A. 1969 Pathological oscillations of a rotating fluid. *J. Fluid Mech.* **35**, 759–773.

TASSOUL, J.-L. 1978 *Theory of Rotating Stars*. Princeton University Press.

TILGNER, A. 1999 Driven inertial oscillations in spherical shells. *Phys. Rev.* E **59**, 1789–1794.

ZAHN, J.-P. 1970 Forced oscillations in close binaries. The adiabatic approximation. *Astr. Astrophys.* **4**, 452–461.

ZHANG, K., LIAO, X. & EARNSHAW, P. 2004 On inertial waves and oscillations in a rapidly rotating spheroid. *J. Fluid Mech.* **504**, 1–40.